
On the Validation of a Code and a Turbulence Model Appropriate to Circulation Control Airfoils

J. R. Viegas, M. W. Rubesin, and
R. W. MacCormack

{NASA-TM-100090} ON THE VALIDATION OF A
CODE AND A TURBULENCE MODEL APPROPRIATE TO
CIRCULATION CONTROL AIRFOILS {NASA} 25 p
CSCL 01A

N88-22864

Unclas
G3/02 0142697

April 1988



National Aeronautics and
Space Administration

On the Validation of a Code and a Turbulence Model Appropriate to Circulation Control Airfoils

J. R. Viegas

M. W. Rubesin, Ames Research Center, Moffett Field California

R. W. MacCormack, Stanford University, Stanford, California

April 1988



National Aeronautics and
Space Administration

Ames Research Center
Moffett Field, California 94035

ON THE VALIDATION OF A CODE AND A TURBULENCE MODEL APPROPRIATE TO CIRCULATION CONTROL AIRFOILS

by

J. R. Viegas and M. W. Rubesin
NASA Ames Research Center, Moffett Field, California, USA

and

R. W. MacCormack
Stanford University, Stanford, California, USA

ABSTRACT

A computer code for calculating flow about a circulation control airfoil within a wind tunnel test section has been developed. This code is being validated for eventual use as an aid to design such airfoils. The concept of code validation being used is explained. The initial stages of the process have been accomplished. The present code has been applied to a low-subsonic, two-dimensional flow about a circulation control airfoil for which extensive data exist. Two basic turbulence models and variants thereof have been successfully introduced into the algorithm, the Baldwin-Lomax algebraic and the Jones-Launder two-equation models of turbulence. The variants include adding a history of the jet development for the algebraic model and adding streamwise curvature effects for both models. Numerical difficulties and difficulties in the validation process are discussed. Turbulence model and code improvements to proceed with the validation process are also discussed.

INTRODUCTION

Code Validation Process

The requirement of validating codes for computational fluid dynamics (CFD) has taken on increased emphasis in recent times. The primary reason for this is that the field of CFD has matured to the point that now it can be considered one of the major tools available to the aircraft designer, namely, an addition and complement to experimental data from wind tunnel and flight tests. However, in order for codes to be used with confidence, designers must know the accuracies and limitations of such a code. The process of establishing these code characteristics has come to be known as code validation.

To the authors, the validation process means developing a computer code whose results agree with the principal aerodynamic data from one or more experiments. These data are the usual force and moment coefficients and visualizations of the flow fields. It is required, however, that the experiments be those with known accuracies and unambiguously defined boundary conditions surrounding the test section, including information on the turbulence intensity and scale at the upstream station. The experiments should also cover a range of variables, such as configurations, Reynolds numbers, Mach number, jet momentum coefficients, etc., that envelop those of the proposed application.

Advances in the development of supercomputers and computational codes have permitted computations, at reasonable costs, of flow field configurations having a complexity approaching that of complete aircraft, when the computations are restricted to inviscid flow. For more realistic physical modeling, configurations such as wing-body combinations can be solved. These advances reflect the considerable improvements that have occurred in techniques for the generation of computational meshes and in solution algorithms in recent years. Currently, there are no inherent limitations on the numerical accuracy that can be achieved with these CFD codes other than their computational expense introduced by additional mesh points and the use of higher order solution techniques. There is a practical limit, however, to which numerical accuracy needs to be driven because all the codes contain certain errors that result from the approximate "physics" which has been introduced into them. For example, panel methods and Euler codes ignore viscous effects and Reynolds averaged Navier-Stokes codes contain only approximate statistical turbulence models. An intelligent use of computer codes has to give consideration to the specific accuracy needs of the designer and, concomitantly, requires an assessment of the errors introduced in the codes by the approximations to the "physics" contained in the codes. Requiring numerical accuracies to be much more stringent than those inherent in the physical aspects of a code is economically unwise and not beneficial to the designer. Thus, the establishment of the magnitude of the errors introduced by various physical approximations over a range of flow variables and configurations is critical to the code validation process. The validation process also serves to uncover lower order logic errors and/or "bugs" that often creep into very large and complex codes and produce subtle, but significant, numerical errors in the results.

In this paper, the initial stages of a validation process are demonstrated with a code that is being developed to compute the performance of circulation control airfoils, where lift is augmented by a surface jet flowing tangentially over the airfoil's blunt trailing edge. The jet adheres to the surface of the airfoil through the Coanda effect. From a turbulence modeling viewpoint the flow over a circulation control airfoil is exceedingly complex, containing such features as surface jets and free shear layers where the jet and the upper boundary layer merge. Each of these regions experience the complicating effects of both high streamwise curvature and adverse pressure gradients. In addition, boundary-layer separation occurs somewhere within the Coanda region where the jet can no longer move forward against an adverse surface pressure gradient. All these effects combine to introduce large pressure gradients normal to the

airfoil surface and recirculation regions, both of which require flow-field solutions to be solved in the Navier-Stokes mode. This paper first describes the development of a computer code that solves the Reynolds-averaged Navier-Stokes equations about the trailing-edge region of a circulation control airfoil in free air. This same code is then extended to apply to an entire airfoil within a wind tunnel test section by including the presence of upper and lower walls. It is this latter arrangement that makes this code particularly suitable for calibration and, ultimately, verification. The code verification process, both in its numerical accuracy and in its turbulence model, can be performed with much less ambiguity because the code can duplicate the wall effects of wind tunnel experiments, provided the flow remains essentially two dimensional. A particularly important experiment such as this has recently been conducted and reported in Ref. 1. Parts of the data of this experiment are used in this paper as standards against which to calibrate the performance of the code with a variety of turbulence models and to suggest the improvements needed in the best of the models. The remaining parts of the available data, that is, the aerodynamic force data over extensive ranges of jet mass flow rates and angles of attack, will be used subsequently to validate the code with the most appropriate turbulence model identified in this initial calibration process.

Computation Method

The computational code employed here uses an extension of the Gauss-Seidel relaxation method proposed by MacCormack in 1985 (Ref. 2). This is an implicit, finite volume method that uses flux splitting. The extensions involve the introduction of second-order space accuracy for the flux-splitting technique and an improved treatment of source terms contained in advanced turbulence models that reinforces the diagonal dominance of their implicit representation and accounts analytically for each of the source contributions (Ref. 3). The resulting code is robust, receptive to different turbulence models, and can use complex mesh arrangements. The acceptability of complex meshes allows the introduction of the wind tunnel walls into the problem, which is critical to the concept of code validation because it allows, in principle, accounting for wind tunnel interference in an unambiguous manner. The code is known to be efficient for flows at transonic and supersonic speeds, but is somewhat slower at the speeds considered here. The latter is a disadvantage in the current work where the improvement of turbulence models requires testing with many repeated runs; however, the ultimate goal of this study is the design of circulation control airfoils operating in transonic flow and for this the code should be effective.

Earlier Results

The earliest application of this code (Ref. 4) was to the experiment of Ref. 5. To save computer time, without sacrificing resolution, the Navier-Stokes computational zone was confined to the immediate region of the trailing edge. The conditions at the boundaries of the zone were estimated from a limited number of velocity measurements, educated guesses of the jet conditions corresponding to the measured mass flow rate, and estimates of total pressures, total temperatures, and flow angles along incoming boundaries and static pressures at outflow boundaries. Subsequently, an analytical potential flow solution for an elliptic cross section airfoil was used to provide the flow angles at the inflow boundaries and static pressures at the outflow boundaries. These boundary conditions and the potential flow solution provided the solution in which the Navier-Stokes zone was immeshed. This surrounding solution will be called the "ambient" solution in the descriptions that follow. Only algebraic models of turbulence (Refs. 6 and 7) and variants required to account for the jet boundary-layer mixing and curvature were used in these calculations. These variants will be described later in the section of this paper entitled Turbulence Modeling. It was found that the computed results were very sensitive to the particular turbulence model employed and to small changes in the estimates of the boundary conditions.

To obtain a firmer understanding of the use of a local Navier-Stokes zone (NS zone) at the trailing edge of a circulation control airfoil, comparisons were next made with the wind tunnel data of Ref. 8. The ambient solution used in this case was provided by the Navier-Stokes computations of Ref. 9. The outer boundary of these computations extended away from the airfoil to distances well beyond the wind tunnel walls, and the effect of the tunnel walls were accommodated by using corrected angles of attack as recommended by the experimentalists. The turbulence model employed in the calculations of Ref. 9 was the Baldwin-Lomax model, but with modifications to account for the intense streamwise curvature in the trailing-edge region of the airfoils. A coefficient in the curvature correction term was altered for each stream velocity and trailing-edge configuration to achieve agreement in lift and surface pressure coefficients with the experimental data (Ref. 8). Thus, the method of Ref. 9 could not be considered predictive in that the "calibration constant" varied from case to case. It was these inadequacies that added an impetus to the current work.

To compute the details of the flow in the trailing-edge region of the airfoil tested in Ref. 8, the local NS zone was imbedded in the ambient solution supplied by the complete Navier-Stokes solution (Ref. 9) as is shown in Fig. 1. The complete Navier-Stokes computation of Ref. 9 was used to define the boundary conditions on the local zone as described previously. On the upstream boundaries these involve the total pressure, total temperature, and flow angles (also the turbulence kinetic energy and dissipation rate if needed by the turbulence model) in the stream and in the jet. The downstream boundary conditions are determined from the static pressure distribution of the ambient solution along the circular boundary. With these boundary conditions there is no assurance that the stream angles on the outflow boundary of the local NS zone would agree with those of the ambient solution at the same location unless the two solution techniques are compatible. To permit focusing on numerical compatibility, an identical turbulence model, Baldwin-Lomax plus curvature correction, was employed in the local zone as was used in the calibrated ambient solution. The test of the compatibility between the two solutions was to adjust the mass

flow rate of the jet entering the local NS zone until the stream angles within the zone at the exit boundary agreed with those of the ambient solution. Note that the mass flow and momentum flow rates in the jet are small compared to those of the inlet or exit boundary, so that changes in the jet conditions from those consistent with the experiment or the ambient calculation of Ref. 9 should not introduce serious mismatches in the conditions at the exit boundary. For the test case of Mach number equal to 0.3, zero geometric angle of attack, a circular trailing edge, and $C_{\mu} = 0.0322$ of Ref. 8, it was found that a reduction of about 10% from the actual jet mass flow rate entering the local computation zone in the ambient solution yielded the agreement in out-flowing streamlines shown in Fig. 2. Here the closely spaced streamlines are from the local zone calculation and the sparse streamlines from the base ambient solution. Thus, the matching procedure, as well as innate differences between the current code and that of Ref. 9, resulted in uncertainties of about 10% in jet mass flow rate required to produce a given lift.

Figure 3 shows a comparison of the experimental pressure coefficients in the Coanda region with the corresponding computed values from the ambient solution code and the immeshed local Navier-Stokes code with the same turbulence model as was used in the ambient solution code and with two additional models. The experimental data from Ref. 8 are designated with open circles, whereas the computed results are shown as solid lines. Figure 3(a) shows this comparison with the computed results of Ref. 9, when the basic turbulence model (Ref. 7) is modified by the calibrated streamwise curvature correction. The agreement in the pressure coefficients is quite good, when consideration is given to the comparatively large spacing between the pressure taps. Figure 3(b) shows a comparison of the data with the computed results of imbedded code calculation, using the same turbulence model as in the ambient calculation, but with 10% less mass flow in the jet. The agreement with the experimental data is almost identical with that of the ambient solution shown in Fig. 3(a). Figure 3 also shows the effect of the turbulence model calibration recommended in Ref. 9. This can be seen in the comparison between Figs. 3(b) and 3(c), where the calibrated curvature correction was removed from the imbedded flow calculation, but with the adjusted mass flow rate of the jet still retained. Removing the curvature correction degrades the accuracy of the computed values. Finally, Fig. 3(d) shows computations with a two-equation model (Ref. 10) without any curvature correction, but with the experimental mass flow rate. These results are also poorer than the case with the "calibrated" reduced mass flow (Fig. 3(b)).

Current Approach

The work just described served to give credence to the current numerical method and suggested continuing its use in developing a turbulence model that did not require alterations for each test condition for the circulation control airfoil. To develop such a turbulence model requires guidance from careful and rather complete experiments, that include measurements of the flow field as well as surface pressure and/or overall forces. Fortunately, an experiment such as this exists (Ref. 1) although it is restricted to fairly low free-stream speeds. The experimenters did not, however, measure profiles of the local flow conditions at the entrance to the wind tunnel test section, and this omission is a cause of concern as will be explained later in this paper. The wind tunnel model in this experiment was large enough to allow some resolution of flow field quantities necessary to define the conditions of the exiting jet and to aid in assessing the performance of the turbulence model. The large size of the model, however, introduced wind-tunnel-wall interference; the tunnel walls were only a few chords away from the wind tunnel model. The experimenters were conscious of the possibility of wind tunnel interference and took care to define the static pressures along the upper and lower walls of the wind tunnel. Thus, to be able to use these data to calibrate codes, guide turbulence modeling and, subsequently, verify the code-model combination, it is necessary to eliminate the uncertainties introduced by the wind tunnel walls by including their presence into the calculation. Since the spiral mesh in the code of Ref. 9 could not do this readily, and also could not accept higher order models easily, it was decided to expand the code developed here from one of a local zone to a complete one that encompasses the entire airfoil and the wind tunnel walls.

CODE DEVELOPMENT

Computation Grid

The grid selected for computing the flow of Ref. 1 is shown in Fig. 4. This grid is generally an O-mesh contoured to fit between the tunnel walls and the airfoil and extends upstream and downstream to the limits of the wall surface pressure measurements. The grid shown contains 126 nodal points in the circumferential direction and 80 in the "radial" direction. This grid can be readily altered locally if more resolution is needed. A unique feature of this grid applied to the circulation control airfoil is that mesh grid lines that emerge from the jet and its lip are allowed to pass forward under the airfoil and then collapse to a singular point at the airfoil leading edge. Details of this mesh in the vicinity of the jet and over the entire trailing edge, or Coanda region, are shown in Figs. 5 and 6. The mesh stretches and shrinks in the outward direction from the body, guided by the need to define the jet region adequately. In the jet, the mesh stretches away from both walls symmetrically. In the mesh shown, 32 points are used to resolve the jet and the jet lip. The mesh behind the jet lip is also stretched, inwardly from the lip surfaces, but is presently fairly coarse, containing 12 points in the mesh shown. It proved to be adequate to assure mesh independent solutions. The mesh contains 48 points stretched from the top surface of the jet lip to the tunnel wall above the jet. Throughout the remainder of the control volume, the mesh stretching described above for the plane of the jet exit is made proportional to the distance from the body to the outside boundaries. Additional test computations were performed with the mesh dimensioned numbers diminished by a factor of 0.7 in both the direction between the airfoil and the

walls and in the circumferential direction. It was found that the results were insignificantly different. It is believed, therefore, that the results shown in this paper are essentially mesh independent.

Boundary Conditions

As previously mentioned, it had been found in the earlier study, Ref. 4, that the computational results for flow about the trailing edge of a circulation control airfoil were very sensitive to the boundary conditions employed. It is felt that this same sensitivity prevails in calculations over the full airfoil, especially when the effects of the tunnel walls are included in the calculations. The flow of Ref. 1 was chosen for this study because it presented the most detailed data available for circulation control airfoil code validation. However, even this well documented experiment contains regions along the boundaries where more complete data would be desired. In the present study, care is exercised to represent the boundary conditions as accurately as possible and with reasonable approximations often substituting for missing information.

No-slip and adiabatic boundary conditions are used on the surface of the airfoil. Slip flow and adiabatic boundary conditions are used on the wind tunnel walls. Subsonic boundary conditions based on the method of characteristics are used at all inflow and outflow boundaries. At the upstream boundary of the control volume, $x/c = -2$, the total pressure, total temperature, and the flow angle are specified. In a complex subsonic flow such as this the influence of the circulation can extend far upstream and downstream of the airfoil. There is evidence in the data of Ref. 1 that this might also be true for this case. Under such conditions, a distribution of total pressure, total temperature, and flow angle would need to be specified everywhere along the upstream boundary to accurately represent the flow entering control volume. For the turbulent field equations, distributions of the kinetic energy and the energy dissipation rate also need to be specified. The latter quantity is extremely difficult to measure, however, profiles of the more easily measured quantities were also not provided in Ref. 1 at this inflow boundary. Thus for the present computations the total pressure and total temperature were taken as constants corresponding to the stagnation chamber conditions for the experiment of Ref. 1. For the low jet momentum case, the pressure on the upper and lower tunnel walls were nearly equal and, consequently, the velocity was assumed to be horizontal along this inflow boundary. For the higher jet momentum case, where the upper and lower wall static pressures were clearly different, the flow angle distribution on the boundary was estimated from a solution of the low-blowing case at a station closer to the leading edge of the airfoil where similar pressure differences existed between the walls. The kinetic energy and the associated energy dissipation rate were assumed constant at values that might correspond to the outer edge of an equilibrium boundary layer at the tunnel test conditions.

At the downstream, or outflow, subsonic boundary, only a precise specification of the static pressure distribution is needed to obtain a solution. The experiment did not provide a pressure distribution in the flow field at this boundary, but the equal tunnel-surface-pressure data at the upper and lower walls at this location suggest that a constant pressure corresponding to their measured values would be reasonable for use on the entire outflow boundary.

At the jet entrance boundary, distributions of the total enthalpy, the mass flux, and the flow angle distributions were specified. These values were estimated from the velocity profiles and flow angles that were provided by the laser doppler velocimeter (LDV) data in the vicinity of the jet exit, as well as from the total jet plenum conditions and the jet mass flow rate. This specification enabled an exact duplication of the jet momentum coefficient, a key parameter in the calibration of circulation control airfoil performance. The kinetic energy and energy dissipation rate distributions in the jet were assumed to be constants equal to the estimated values in the free stream at the entrance to the tunnel test section. This assumption and possible consequences are discussed more fully in the next section.

The computations were initiated by assuming no flow throughout the control volume and applying the tunnel total conditions at the entrance and tunnel static pressure at the exit. The jet is gradually introduced by controlling the mass flow rate. From this gentle start the flow relaxes smoothly, but sometimes with a persistent, but damped oscillation, to convergence.

Turbulence Modeling

Although it is known (Ref. 11) that full second-order, Reynolds-stress turbulence modeling captures the anisotropies and related reduction of skin friction that develop over convex curved surfaces such as exist at the trailing edge of a circulation control airfoil, this level of modeling is currently too costly in terms of algorithm derivation and computer run times to be considered at the current stage of development of the present computer code. Consequently, the turbulence models used in this study employ the simplifying concept of an eddy viscosity.

The basic turbulence models that were used here fall into two categories. The first is an algebraic model, developed by Baldwin-Lomax (Ref. 7). The second is the two-equation model, developed by Jones and Launder (Ref 10). As these models are most appropriate for ordinary attached boundary layers, variations of each of these models were also employed to account for the history of the development of the free shear layer between the jet and the upper surface boundary layer for the case of the algebraic model, as described later, and/or for the extreme streamwise curvature of the trailing and leading edges in both models.

The LDV data of Ref. 1 indicate that the boundary layers approaching the trailing edge region on both the upper and lower surfaces of the airfoil are turbulent. The experimenters tripped the boundary layer

at $x/c = 0.075$ on the lower surface, and suggest that transition to turbulence also occurred on the upper surface very close to the leading edge. For these reasons, the turbulence was assumed to occur from the leading edge for the algebraic models. For the two-equation model, transition to turbulence occurs automatically when free-stream turbulence is introduced, although the location and extent of transition is not necessarily physically correct. For this model, the calculations indicate transition is complete by $x/c = 0.05$ on the upper surface, but as late as $x/c = 0.4$ on the lower surface. It is expected, however, that this late transition on the lower surface will have only a secondary influence on the overall behavior of the circulation control jet.

Recall that the Baldwin-Lomax model, which is divided into two zones, treats the inner zone with the van Driest form of the mixing length, which increases monotonically with distance from the surface. The extent of the inner zone is determined by the location of the point where the product of the distance from the surface and the absolute value of the local mean vorticity first becomes a maximum. The size of the eddy viscosity over much of the boundary layer is established by the value of the eddy viscosity at this point. In the region over the trailing edge where the presence of the jet is still distinct, this maximum occurs very close to the surface, well below the point of maximum velocity in the jet. Since the total jet height in the experiment of Ref. 1 is only approximately 5% of the upper-surface boundary-layer thickness at the lip of the jet, it is seen that the Baldwin-Lomax model applied to the jet boundary layer interaction largely ignores the much larger scales of the entrained boundary layer. Thus, the eddy viscosity in the free-interaction zone between the surface jet and the boundary layer as given by the Baldwin-Lomax model can be expected to be too low, which limits mixing with the free shear layer and in turn permits the surface jet to maintain larger velocities as it moves around the trailing edge; however, the eddy viscosities near the surface, below the position of the maximum velocity in the jet are scaled properly. When combined with the faster moving jet, these proper eddy viscosities allow separation to occur farther downstream.

To assess the importance of this apparent deficiency of the Baldwin-Lomax model, the basic model was modified to account for the distribution of the eddy viscosities within the jet at its exit and the boundary layer above the jet lip. Within the jet, these eddy viscosities were established by assuming the jet to behave as two boundary layers separated by an inviscid core. This assumption was found to be consistent with the total mass flow rate of the jet and the laser doppler velocities as measured in the experiment of Ref. 1. In the top surface boundary layer at the lip of the jet exit, the eddy viscosities were established as part of the overall computation process. To account for the "history" of the jet development, these eddy viscosities at the jet exit station were then blended with the local eddy viscosity given by the Baldwin-Lomax model through a linear weighting function that gave full weight to the upstream values at the jet exit and full weight to the Baldwin-Lomax model at the trailing edge. No attempt was made to optimize the length of the region of blending. The process was used only to gain some insight into the effects of the apparent shortcomings of applying the Baldwin-Lomax model to the present problem. Corrections for the effects of streamwise curvature were made as recommended in Ref. 9.

With the two-equation model, the interaction of the jet and boundary layer proceeds as part of the overall solution process. In contrast to the mixing length model, no new modeling in the jet-boundary layer interaction zone was required. It was necessary, however, to define boundary conditions for the kinetic energy and energy dissipation rate at the exit plane of the jet. The laser doppler data of Ref. 1 show rather intense turbulent kinetic energy emerging from the jet, however, no consistent way could be found to estimate the corresponding kinetic energy dissipation rate at the jet exit. To permit proceeding with the solution of the two-equation model, it was decided to bypass the problem of arbitrarily assigning dissipation rates to the measured kinetic energies by merely assuming that the values of the kinetic energy and dissipation rate at the jet exit were the same as was estimated at the inflow boundary of the wind tunnel test section. Although this appears to be a rather poor assumption, it is not believed that it introduces serious error in the solutions because it was noticed that both the kinetic energy and dissipation rates increased very rapidly downstream of the jet exit to values consistent with those that occur within shear layers. Future studies will examine the sensitivity of the solutions to altered assumptions regarding the turbulence conditions at the jet exit.

To account for the intense streamwise curvature in the Coanda region, the methods of modifying the two-equation model for curvature recommended in Ref. 12 were adopted here. In this method the coefficient in the destruction term of the dissipation equation is modified by a correction factor equal to one minus a curvature coefficient times a Richardson number. The modeling coefficient accounting for curvature was set equal to the recommended value of 0.2. The radius of curvature employed in the Richardson number was set equal to that of the surface of the model, not local values along the streamlines. This was done for expediency; however, it is not believed to introduce serious error because those regions where the tangential jet plays its most important role are quite close to the body surface. Because the streamwise curvature terms are meant to be perturbations to uncorrected models of turbulence, the curvature correction factor was restricted to values between 0.25 and 1.75.

RESULTS

Test Conditions

The computations shown in this paper apply to the experimental conditions of Ref. 1 where both flow field velocities and surface pressures were measured. In particular, computed results are presented for the following:

Test section conditions:

Velocity, $U = 42.50$ m/s
 Chord Reynolds number = 10^6
 Free-stream Mach number = 0.121
 Total temperature = 303.2 K
 Total pressure = 98952.0 N/m²

Model conditions:

Chord of airfoil, $c = 0.382$ m
 Angle of attack = 0°
 Dimensionless jet height, $h/c = 0.002$
 $U_{jet}/U_{free\ stream} = 3.44$ and 5.69
 Jet momentum coefficient, $C_\mu = 0.03$ and 0.1

Although Ref. 1 contains airfoil surface pressure data over a range of angles of attack from -5° to +5°, and includes jet momentum coefficients up to about 0.4, the computations shown here were confined to those just indicated because it was under these conditions that LDV measurements were made in the trailing-edge region. These velocity measurements were used in the computations to define the mean flow conditions at the jet exit, and as standards for comparison with the computed results. Of course, in the final validation process of the computer code with its best turbulence model, the entire range of the test conditions of Ref. 1 should be computed and the results compared with the surface pressure data, lift, drag, and pitching moments.

Example of Flow Field Results

Figures 7 through 9 show examples of the flow fields computed about the circulation control airfoil in the wind tunnel test section. This group of computations is based on the unmodified Baldwin-Lomax model and apply to the lower jet momentum coefficient equal to 0.03. Figure 7 shows the streamlines about the airfoil within the entire test section. The overall effect of the circulation control jet is evident in the downwash shown at the trailing edge and in the upwash at the leading edge that is induced by the circulation that has been created. It is significant that a larger proportion of the wind tunnel airflow passes over the airfoil than underneath, and is an indication that wind tunnel wall interference is likely to be important in these experiments.

It should be noted that the plotting routine used here has difficulty in accounting for the presence of the jet in evaluating the absolute numerical values of the streamlines because of a local new source of mass. Accordingly, the lines shown should be considered to be streaklines. The specific numbers on the lines are not proper stream function values and are used here merely as line identifiers. The anomalous behavior can be seen in the enlarged figures as stagnation lines that do not meet the surface of the airfoil or those that are inconsistent with the velocity vectors near the trailing edge. Farther from the airfoil surface the streaklines agree quite well with the corresponding velocity vector fields.

The details of the flow field in the leading-edge region are shown in the expanded plots of Fig. 8, where (a) shows the streamlines and (b) shows the velocity vector field. The latter figure indicates that the stagnation point occurs at about 2% of chord on the lower surface of the airfoil. The velocities passing over the leading edge to the upper surface are much larger than the free stream values and suggest considerable leading edge suction. There is no evidence of a leading-edge separation bubble on the upper surface.

Similar detailed flow field results are shown at the trailing edge in Fig. 9. On Fig. 9(a), the streamline labeled 0.00, away from the surface of the body, is approximately the lower bound of the free-stream air passing over the top of the airfoil. It shows that the trailing edge jet hugging the surface is effective in inducing considerable downwash at the trailing edge. The presence of the jet is very evident in Fig. 9(b), and it can be seen to exist well around the trailing edge. It should be noted, however, that the jet has separated from the surface a short distance ahead of the trailing edge. This cannot be seen clearly from the figure, but is detected in the calculated skin friction directions.

Comparative Turbulence Model Performance

Figure 10 and Table 1 show the computed predictions of the the lift coefficients in comparison with the experimental results of Ref. 1. The lift data were obtained in Ref. 1 from integration of the experimental pressure distributions about the airfoil. The calculated lift was computed in a similar way from the local calculated surface pressures. For this paper, most of the airfoil computations were performed for the jet momentum coefficient equal to 0.03, with just one case shown for $C_\mu = 0.1$. Recall these were the jet conditions where laser doppler measurements were made of the trailing edge flow field in addition to surface pressure measurements on the model. The turbulence models indicated here were described in a previous section.

It is observed from the figure and the table that the basic Baldwin-Lomax turbulence model yields results that are approximately 50% higher than the data at each value of the jet momentum coefficient. Including the effect of the jet history causes the lift to rise. The reason for this is that the jet at its exit, as assumed in the calculations, possesses quite a low value of eddy viscosity relative to that which the Baldwin-Lomax model would predict for the stations downstream of the jet exit. Consequently, the weighting procedure adopted to account for the jet history lowers the eddy viscosities in the free

shear layer between the jet and the overlaying boundary layer. The result of this is to reduce the mixing and, hence, the retardation of the jet and to allow it to move farther around the Coanda region. Alternatively, the near wall eddy viscosities are not affected much by the jet history weighting. The combined effect of less jet retardation and similar eddy viscosities in the vicinity of the wall cause the point of separation to move farther around the trailing edge, which in turn, contributes to the increased lift. It is interesting that the Jones-Launder model yields essentially the same results, which indicates that the history effects that are inherent in the two-equation model were fortuitously approximated with the weighting procedure adopted here for the Baldwin-Lomax algebraic model.

The effect of the curvature correction in the algebraic model is to reduce the lift. With the value of the curvature correction coefficient, C_c , introduced in Ref. 9 set equal to 8.0, it is found that the lift is still about 37% higher than the experimental value at $C_\mu = 0.03$. The reason for the reduction of lift introduced by the curvature correction is that it reduces the eddy viscosity between the maximum velocity in the jet and the wall, while generally increasing the eddy viscosity in the interaction zone between the jet and the exterior flow. Thus, the jet is retarded more by the external flow and increasingly susceptible to separation. These effects combine to move the separation point towards the jet exit and result in a reduction of the overall lift. To approach the experimental data by reducing the lift even more, some runs were made with the code with values of $C_c = 10.0$ and 12. It was found that the increment of reducing the lift diminished and that some periodic oscillations were introduced into the solution. Also, these values of C_c are an order of magnitude larger than those required in Ref. 9 to achieve agreement with the data of Ref. 8. It is believed that the difference in the way the two codes behaved in their comparisons with the different experiments was primarily the result of the freedom enjoyed in Ref. 9 of also being able to adjust the angle of attack. Because of inherent weaknesses of the Baldwin-Lomax model's ability to handle the complexities of this flow, we did not pursue this matter further at this time.

The last modification made to the Baldwin-Lomax model was to combine the effects of jet history and curvature. As expected, the effects tended to cancel and resulted in values of lift close to that of the original Baldwin-Lomax model. The Jones-Launder two-equation model, corrected for curvature as in Ref. 12, also yields results that are quite similar to those of the original Baldwin-Lomax model, or its variants that contain curvature corrections. This conclusion is not unique to the circulation control airfoil, but has also been demonstrated in the computation of transonic airfoils without curvature corrections (Ref 13). For a circulation airfoil, then, the only advantage of using the Jones-Launder two-equation model is its ability to account for the jet history without additional modeling assumptions. It is known that the performance of the Jones-Launder model can be improved considerably, and procedures for doing this are listed later in the description of the future directions this code validation process may take.

The streamline patterns in the trailing edge region of the circulation control airfoil corresponding to the different variants of the Baldwin-Lomax model are shown in Fig. 11. These are in agreement with the explanations given above for the behavior of the lift, and can be seen best by comparing the positions of the streamline labeled 0.01 in Figs. 11(a) to 11(c). With reference to Fig. 11(a), corresponding to the basic Baldwin-Lomax model, the streamlines in Fig. 11(b), including the effects of jet history, show a decided movement clockwise around the trailing edge which is reflected in increased lift. The curvature correction alone, Fig. 11(c) shows a counter-clockwise movement relative to Fig. 11(a). Finally, the combined effects of jet history and curvature corrections, as shown in Fig. 11(d), bring the streamline pattern almost back to its original form (Fig. 11(a)).

Figure 12 shows the flow field in the trailing-edge region corresponding to the smaller jet-mass coefficient, $C_\mu = 0.03$, when the basic Jones-Launder two-equation model is used. As expected from the comparisons of the results for lift, the stream pattern shown in Fig. 12(a) is virtually identical with that of Fig. 11(b), corresponding to the Baldwin-Lomax model with jet history. The vector plot (Fig. 12(b)) shows separation to occur on the surface of the airfoil just beyond the trailing edge in a clockwise direction. It is remarkable how large a "dead water region" (i.e., very low velocity) exists just below the trailing edge. The relatively large spacing between the streamlines labeled 0.000 and 0.016 on Fig. 12(a) are also indicative of this.

A comparison of Figs. 12(a) and 12(c) shows the effect of the curvature correction on the Jones-Launder model on the streamline pattern in the trailing-edge zone. Near the surface, the curvature correction introduces a decided counter-clockwise motion to the flow field. In addition, there is significantly less downwash in the far field. The vector fields, shown in Figs. 12(b) and 12(d), support these observations and give more detail of the jet behavior near the surface. The identity of the jet remains evident to farther clockwise positions without the curvature correction. This flow pattern behavior is consistent with an increase in the jet-free stream mixing and a significant reduction in the lift as a result of the curvature correction.

Figure 13 shows the streamline pattern around the entire airfoil corresponding to the basic Baldwin-Lomax model for the two values of jet momentum coefficient used here. Figure 13(a) is a blowup of the streamline pattern shown earlier in Fig. 7 for $C_\mu = 0.03$. Figure 13(b), corresponding to $C_\mu = 0.1$, shows how dramatically the flow under the entire airfoil is affected by the increase in the jet momentum coefficient. The air exiting the jet is seen to circulate about the airfoil. The air that originally passes over the upper surface of the airfoil is thrown forward under the airfoil to about 20% chord by the circulation control jet. The complexities of this flow certainly tax the bases of the Baldwin-Lomax model, the only one used to date for this flow condition.

Figure 14 shows a comparison of the computed and measured trailing-edge mean streamline patterns for both values of the jet momentum coefficient. The computations shown in these figures are based on the Baldwin-Lomax model, without modifications. Figure 14(a) is a more detailed version of Fig. 11(a), corresponding to a value of jet momentum coefficient, $C_{\mu} = 0.03$. Figure 14(b) is the corresponding figure for $C_{\mu} = 0.1$. Figures 14(c) and 14(d) show the experimental results from Ref. 1 for the same pair of values of jet momentum coefficient. Recall, now, that the experimental lift produced by the value of $C_{\mu} = 0.03$ is much less than that corresponding to the computation for the same value of C_{μ} . The experimental lift for $C_{\mu} = 0.1$ also is much less than the computed lift; however, it is above the computed lift for the case of $C_{\mu} = 0.03$, see Table 1. The patterns of the flow fields in Figs. 14(a), (b), and (d) are generally consistent with these observations. The experimental flow pattern for $C_{\mu} = 0.1$, except for exhibiting some waviness, generally lies between the two computed patterns. Some features appear in the streamline pattern of Fig. 14(c) that are inconsistent with the lift behavior. Although in the immediate vicinity of the surface, the experimental streamlines turn less clockwise than the computed values shown in Fig. 14(a), consistent with the relative lifts, the experimental flow pattern away from the surface indicates more downwash than does the computation. Why this is not reflected in more experimental lift is not clear at this time and will require further study and interaction with the experimenters, as will the anomalous results shown in the next figure.

Figure 15 shows comparisons of the measured pressure coefficients on the upper and lower surfaces of the airfoil in comparison with some of the computations. Figure 15(a) compares the experimental data (circular symbols), with computed results (solid lines) based on the Baldwin-Lomax model containing corrections for curvature for the same values of jet momentum coefficient, $C_{\mu} = 0.03$. Figure 15(d) shows a similar comparison for the Jones-Launder model, with curvature correction. These alternative model comparisons are virtually identical. The oscillations in the computed quantities on the upper surface near the leading edge are believed to have resulted from the first-order curve-fitting procedure employed to interpolate between the wind tunnel model coordinates in setting up the airfoil surface coordinates for the computation mesh. It is not believed that these oscillations seriously impair the global results or the conclusions that can be drawn therefrom. The larger computed lift, noted earlier, is shown by the larger area between the upper and lower lines than exhibited by the area bounded by the experimental points. In addition, it is shown here that a large part of the increased lift evident in the computed results occurs over the forward portion of the airfoil. The computed drag and pitching moments also will differ considerably from the measured values because of this behavior.

The cause of the large leading-edge suction pressure shown in the computations and absent in the data is critical to our understanding of the directions future turbulence modeling modifications should take for this class of flow. Towards this end, it was decided to compare computations with data at the same lift, accomplished by comparing with experimental data at a higher jet momentum coefficient that provides the proper lift. From Fig. 10 it is seen that such a match exists with the computations of the Baldwin-Lomax model with jet history or the basic Jones-Launder model with $C_{\mu} = 0.03$ and the experimental data at $C_{\mu} = 0.62$. The comparisons of pressure coefficients from these computations and the experimental data are shown in Figs. 15(b) and 15(c). First, it is striking how closely the results for the two turbulence models agree in these figures. In each figure, the apparent area between the computed lines now agrees more closely with the area between the groups of data points. As in Fig. 15(a), but to a lesser extent, on the upper surface, the computed pressure coefficient shows more of a suction peak in the vicinity of the leading edge than is exhibited by the data. At the trailing edge, less suction is generated. It is clear that an improvement in the turbulence model that would achieve the correct suction peak in the trailing-edge region, at the proper or matched lift, would be helpful in reducing the leading edge suction peak. This interplay of the behavior of the leading-edge and trailing-edge flow regions was not evident in the earlier work (Refs. 8 and 9). In the calculations of Ref. 9, "wind tunnel corrections" to the actual geometric angle of attack, as recommended by the experimenters of Ref. 8, were introduced simultaneously with turbulence model changes to improve the pressure coefficient behavior in the leading edge region. In the current work, with the inclusion of the wind tunnel walls in the calculations, in principle one should not be justified in modifying geometrically established angles of attack. The burden should be on the improvement of the turbulence model so that results, to the accuracy required by the user, are attained when ambiguities in the boundary conditions are minimized or assessed. For example, Fig. 16 shows the calculated upper and lower wind tunnel wall static pressure coefficients corresponding to the case where $C_{\mu} = 0.03$ with the Jones-Launder turbulence model and some representative experimental measurements. The differences in the pressure coefficients at the upstream boundary indicate the extent of the upstream influence on the flow caused by the circulation. Recall that only the total pressure was assigned at this boundary and these static pressure differences developed as part of the solution. Differences between the measured and calculated static pressures at this station would suggest that the assumption of zero angle of flow for the incoming streamlines, employed in the calculations with $C_{\mu} = 0.03$, may have introduced some error. This is an example where more complete documentation (i.e., stream angles at the entrance to the test section) would have eliminated some degree of uncertainty in the calculations.

Before leaving this section, it should be mentioned that none of the solutions described were easily obtained. The algorithm, developed for compressible flows, seemed to be taxed by the complex low subsonic flow studied here. Even though the algorithm is robust (in that once debugged, it could be operated with very large time steps or CFL numbers, as befitting a good implicit code) there was a problem obtaining quick convergence for the circulation control airfoil at all the conditions studied. During the relaxation process from an initial flow condition towards a new steady state, the solution would oscillate very slowly with no apparent physically based characteristic frequency. The oscillation was related more to

the number of iterations, as seen by comparisons at different values of CFL number. The magnitude of the oscillations sometimes seemed dependent on the size of the CFL number. On some occasions, the oscillations persisted indefinitely. The solution behaved as if the feedback between the various boundaries made the equation set very stiff. The overall lift was the aerodynamic parameter focused upon, and for the solutions present, this parameter converged to within 1%, even in the presence of oscillations. The number of iterations required to attain this convergence level could be from several hundreds to a few thousand. The larger number of iteration counts was required when the jet momentum coefficient was the low value of $C_{\mu} = 0.03$. At the higher value of $C_{\mu} = 0.1$, the convergence rate of a few hundred iterations is very respectable. Currently the code is unvectorized and computations cost 10 to 15 sec/iteration on a Cray XMP for the algebraic and two-equation turbulence models, respectively. Increased computational efficiency, while not critical, is certainly worth pursuing to enhance the code's efficiency at the lower free stream speeds and lower jet momentum coefficients.

Although the 1% oscillation in lift, the overall flow pattern, and the friction drag indicated the solutions had achieved an acceptable level of convergence, other aerodynamic parameters such as the pitching moment or the pressure drag, because of their dependence on relatively small differences between large quantities, continued to show disproportionately large oscillations. It is expected that improving the numerical fit to the body shape and grid about the leading edge of the airfoil will reduce the raggedness of the surface pressure in this region shown in Fig. 15. The improved grid may also reduce the range of the oscillation of the higher order aerodynamic parameters.

CONCLUDING REMARKS

This paper presents the early stages in a program to calibrate and validate a computer code being developed to compute the performance of circulation control airfoils. The opportunity to attempt this validation process arose because of 1) the availability of new data from an experiment that included mean flow and turbulence measurements in addition to model surface pressure data (Ref. 1), and 2) the development of a computer code that could account for the presence of a model within wind tunnel walls, with the latter experiencing slip flow conditions. The code is currently two-dimensional, requiring the model to be an airfoil, and only accounts for the upper and lower wind tunnel walls. The computer code is also capable of accepting different kinds of turbulence models, both algebraic or those based on auxiliary field equations for turbulence quantities. Finally, the code, which is known to be economical for high-speed compressible flows (Ref. 2) has proven to be only marginally economical for this low-speed flow condition at the lower jet momentum coefficient. Under these conditions, the code presently is useful only as a research tool when enough mesh points are employed to provide numerical results that are mesh independent.

Inclusion of the wind tunnel walls in the calculations was expected to eliminate some of the uncertainties introduced by empirical wind tunnel wall "corrections" and to place the burden squarely on the turbulence models to achieve an agreement between computations and experimental data, provided adequate boundary condition data are known for the incoming and outflowing boundaries of the test section. The present computed results, which show higher suction pressures at the leading edge and less downwash beyond the trailing edge than indicated in the experimental data, even when total lift is matched to the experimental results, are indicative of a negative effective angle of attack. The cause of this anomalous behavior is not known at this time, but could result from an induced three-dimensional effect that was not detected in the experiment and could not be generated by the present two-dimensional flow code.

Despite these aforementioned uncertainties regarding the effects of undefined conditions on the test section boundaries and the apparent residual angle of attack, even in the presence of the computed wall effects, and the relatively uneconomical behavior of the compressible flow code applied to low speeds, the current study provided several positive results regarding the process of validating a code for the design of circulation control airfoils. Some of these are as follows:

1. Computations applying turbulence models that are used commonly in Navier-Stokes codes, namely, the Baldwin-Lomax algebraic model and variants to account for curvature and the history of jet merging with the external flow field or the Jones-Launder k-epsilon model with corrections for streamwise curvature, show little difference between each other and both provide good qualitative descriptions of the flow fields about the circulation control airfoil.
2. The code proved to be readily adaptable to higher order turbulence modeling, and the cost penalty of running the two-equation model relative to the zero equation model was only an increase of 50%.
3. The code converged sufficiently rapidly if the initial conditions were a previous solution at somewhat different flow conditions or with a different turbulence model. It was also noticed that convergence occurred quite rapidly at the high value of the jet momentum coefficient. These characteristics should be useful in parametric studies involved in the ultimate validation process under low-speed conditions.
4. The code is written in a generalized coordinate frame. This feature allowed generation of the mesh involving the airfoil and wind tunnel wall to be very direct, and should be easily adapted to include geometric angles of attack. This will be needed to investigate the apparent angle of

attack evident in the experimental data and to allow covering the range of angle of attack measured in Ref. 1.

5. For the limited cases computed to date, the turbulence models employed indicate quantitative results that, for given jet mass coefficients, show values of lift that are approximately 50% too high at both values of jet mass flow that have been computed. This suggests that the code could possibly be "calibrated", but such a task requires computation at other test conditions to confirm the concept.

With these results, decisions have to be made how to proceed in advancing the validation of this code. Should one try to calibrate the code over the entire range of conditions for which experimental data exists, even though it is apparent that the calibration may involve large, and possibly non-uniform, adjustments to the computed results? Or should one try to first eliminate the uncertainties in the boundary conditions through consultation with the experimenters and then improve an existing turbulence model, or obtain a new turbulence model, to yield values of all the aerodynamic coefficients that are close and consistent with trends of a limited set of experimental data? This second approach, if successful, could enable one to proceed with confidence with the validation process over the ranges for which the circulation control airfoil has been tested.

The authors agree with the latter of these two philosophies, but are aware of the difficulties in advancing a turbulence model to flow conditions that are large extrapolations beyond the conditions of the fundamental fluid dynamic experiments upon which the current models utilized here were based. In the present example, such experiments involved surface jets on planar or curved surfaces, and free shear layers between surface jets and boundary layers; however, the radii of surface curvature and pressure gradients were orders of magnitude less influential than those which exist in the trailing edge of a circulation airfoil. Thus, it is not surprising that the models employed in the present paper were not adequate for design.

The authors are continuing to develop the computer code. In the near future, the following numerical and turbulence modeling modifications will be tried:

1. Close attention will be placed on obtaining a smooth body contour at the leading edge to eliminate this as source of numerical problems.
2. Numerical algorithm improvement for low-speed conditions is still warranted and is being pursued.
3. Sensitivity studies will be conducted with variations in the stream angles entering the test section and with small changes in the angle of attack. (The reasonableness of the magnitudes of the quantities used in the sensitivity studies will be checked through consultation with the authors of Ref. 1.)
4. Sensitivity studies with the Jones-Launder model plus curvature will be conducted to test the need for defining the turbulence, in scale and intensity, at the exit plane of the jet.
5. Wall functions will be introduced to the Jones-Launder model. These were found to help the Jones-Launder model in transonic flows (Ref. 14) and in subsonic deadwater regions (Ref. 15).
6. The Jones-Launder model will be modified to account for the effects of streamwise curvature by reinterpreting the kinetic energy equation to account for anisotropy in a manner similar to what was done in Ref. 11.
7. The Jones-Launder model will be modified to relax the eddy viscosity concept through the use of Rodi's algebraic stress model (Ref. 16).
8. Full Reynolds stress modeling will be introduced in the manner of Ref. 3.

At present it is not clear what level of modeling will lead to results that are reasonably accurate and characteristic of the behavior of changes in the data with alterations in the flow conditions to warrant fine tuning through calibration. Success here, will lead to testing the code over the entire range of conditions of the experiment of Ref. 1 and for a new experiment being conducted at the NASA Ames Research Center that will extend the data, similar to that obtained in Ref. 1, to a circulation control airfoil within a transonic flow.

Although Ref. 1 was well written, it was found during the computations described here that occasions arose when consultation was required with the authors of that paper to clarify some of the experimental conditions. The excellent cooperation given by these experimentalists was extremely beneficial to the current work and is a demonstration of the strong need for close cooperation between experimentalists and code validators that should be a continuing process for future studies.

REFERENCES

1. Novak, C. J., Cornelius, K. C., and Roads, R. K., "Experimental Investigations of the Circular Wall Jet on a Circulation Control Airfoil," AIAA-87-0155, AIAA 25th Aerospace Sciences Meeting, Reno, Nevada, January 12-15, 1987.
2. MacCormack, R. W., "Current Status of Numerical Solutions of the Navier-Stokes Equations," AIAA-85-0032, AIAA 23rd Aerospace Sciences Meeting, Reno, Nevada, January 14-17, 1985.
3. HaMinh, H., Kollmann, W., and Vandromme, D., "Implicit Treatment of Multi-Equation Turbulence Models for Compressible Flows," Final Report for Contract NASA-NCC2-186, University of California, Davis, Calif., 1987.
4. Viegas, J. R., Rubesin, M. W., and MacCormack, R. W., "Navier-Stokes Calculations and Turbulence Modeling in the Trailing Edge Region of a Circulation Control Airfoil," Circulation Control Workshop, NASA Ames Research Center, Feb. 19-21, 1986.
5. Spaid, F. W. and Keener, E. R., "Boundary Layer and Wake Measurements on a Swept, Circulation Control Wing," Circulation Control Workshop, NASA Ames Research Center, Feb. 19-21, 1986.
6. Cebeci, T. and Smith, A. M. O., Analysis of Turbulent Boundary Layers, Academic Press, New York, 1974.
7. Baldwin, B. and Lomax, H., "Thin-Layer approximation and Algebraic Model for Separated Turbulent Flows," AIAA-78-257, 1978.
8. Abramson, J. and Rogers, E. O., "High-Speed Characteristics of Circulation Control Airfoils," AIAA-83-0265, AIAA 21st Aerospace Sciences Meeting, Reno, Nevada, January 10-13, 1983.
9. Pulliam, T. H., Jespersen, D. C., and Barth, T. J., "Navier-Stokes Computations for Circulation Controlled Airfoils," AIAA-85-1587, AIAA 18th Fluid Dynamics and Plasmadynamics and Lasers Conference, Cincinnati, Ohio, July 16-18, 1985.
10. Jones, W. P. and Launder, B. E., "The Prediction of Laminarization with a Two-Equation Model of Turbulence," International Developments in Heat Transfer, Vol. 15, 1972, pp. 303-314.
11. Wilcox, D. C. and Rubesin, M. W., "Progress in Turbulence Modeling for Complex Flow Fields Including Effects of Compressibility, NASA Technical Paper 1517, April 1980.
12. Launder, B. E., Priddin, C. H., and Sharma, B. I., "The Calculation of Turbulent Boundary Layers on Spinning and Curved Surfaces," Transactions of the ASME, Journal of Fluids Engineering, pp. 231-239, March, 1977.
13. Rubesin, M. W. and Viegas, J. R., "Turbulence and Modeling in Transonic Flow," Transonic Symposium, Theory, Application, and Experiment, NASA Langley Research Center, Hampton, Virginia, April 19-21, 1988.
14. Viegas, J. R., Rubesin, M. W., and Horstman, C. C., "On the Use of Wall Functions as Boundary Conditions for Two-Dimensional Separated Compressible Flows," AIAA-85-0180, AIAA 23rd Aerospace Sciences Meeting, Reno, Nevada, January 14-17, 1985.
15. Chen, H. C. and Patel, V. C., "Practical Near-Wall Turbulence Models for Complex Flows Including Separation," AIAA-87-1300, AIAA 19th Fluid Dynamics, Plasma Dynamics and Lasers Conference, Honolulu, Hawaii, June 8-10, 1987.
16. Rodi, W., "A New Algebraic Relation for Calculating the Reynolds Stresses," ZAMM, Vol. 56, 1976.

ACKNOWLEDGMENT

The authors wish to acknowledge the excellent cooperation provided by the staff of the Advanced Flight Sciences Department of the Lockheed-Georgia Corporation, in particular, Mr. C. J. Novak, in providing unpublished wind tunnel data of the experiment described in Reference 1.

R. W. MacCormack acknowledges the support by NASA Ames Research Center, through Joint Research Interchange No. NCA 2-40.

TABLE 1
COMPARISON OF EXPERIMENTAL AND COMPUTED LIFT COEFFICIENTS

SOURCE	JET MOM. COEFFICIENT, C_μ	LIFT COEFFICIENT, C_L	ERROR, %
EXPERIMENT	0.03	1.50	
COMPUTATIONS			
BALDWIN-LOMAX (BL)	0.03	2.26	+51
BL + HISTORY	0.03	2.51	+67
BL + CURVATURE CC = 8.0	0.03	2.06	+37
BL + CURVATURE + HISTORY	0.03	2.24	+49
JONES-LAUENDER (JL)	0.03	2.54	+69
JL + CURVATURE	0.03	2.08	+39
EXPERIMENT	0.10	3.58	
COMPUTATIONS			
BL	0.10	5.30	+48

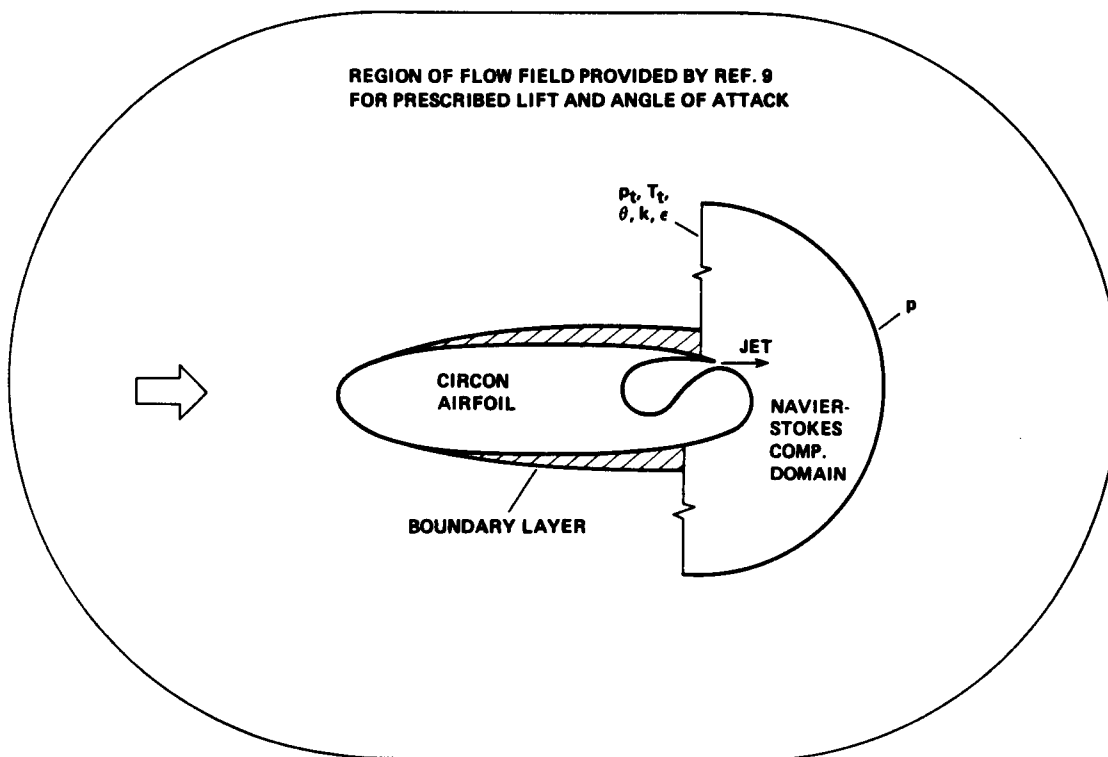


Figure 1.- Sketch showing procedure employing a local computational zone at the trailing edge of a circulation control airfoil.

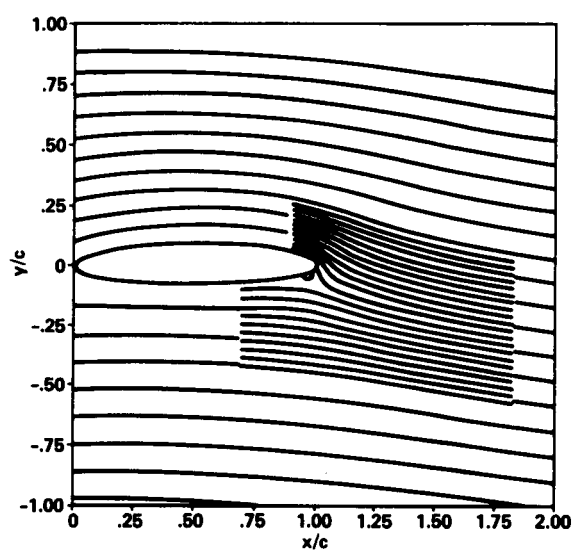


Figure 2.- Overlay of streamlines from local zone calculation onto those of ambient calculation of reference 9.

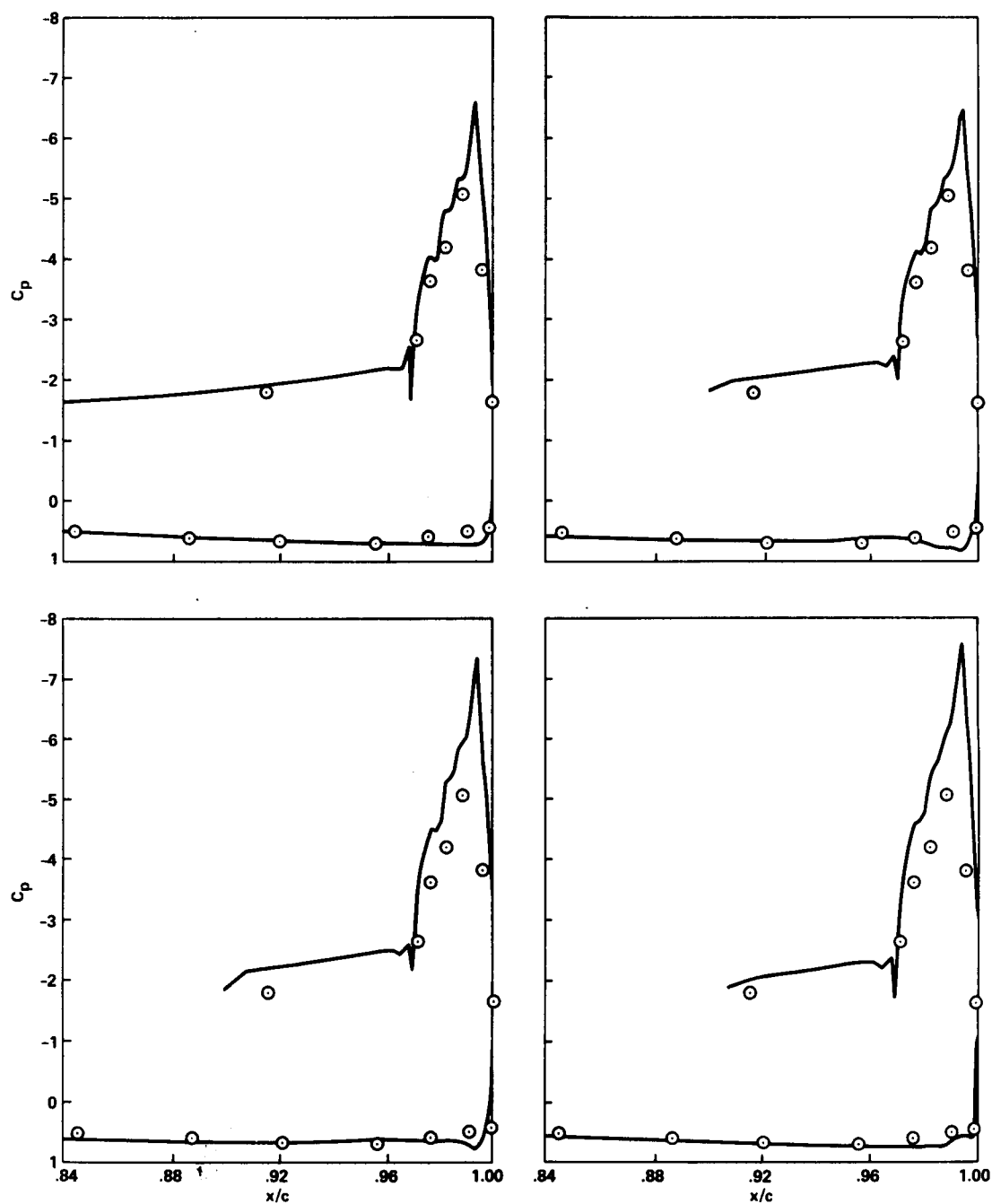


Figure 3.- Surface pressure coefficients on the trailing edge of the circulation control airfoil of reference 8. a) Full field solution of reference 9, Baldwin-Lomax turbulence model plus curvature correction. b) Local Navier-Stokes solution, Baldwin-Lomax turbulence model plus curvature correction. c) Local Navier-Stokes solution, Baldwin-Lomax turbulence model, no curvature correction. d) Local Navier-Stokes solution, Jones-Launder turbulence model, no curvature correction.

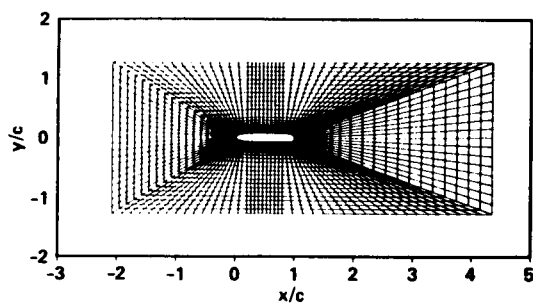


Figure 4.- Grid used for full airfoil/test section computation.

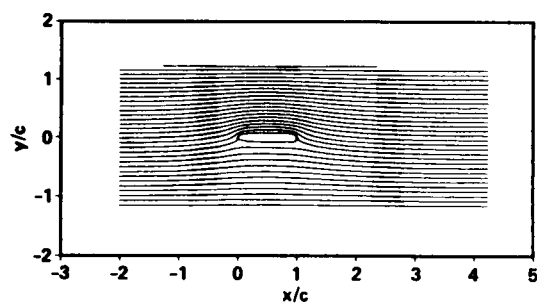


Figure 7.- Stream function of flow field in test section with circulation control airfoil. Baldwin-Lomax turbulence model; $C_\mu = 0.03$.

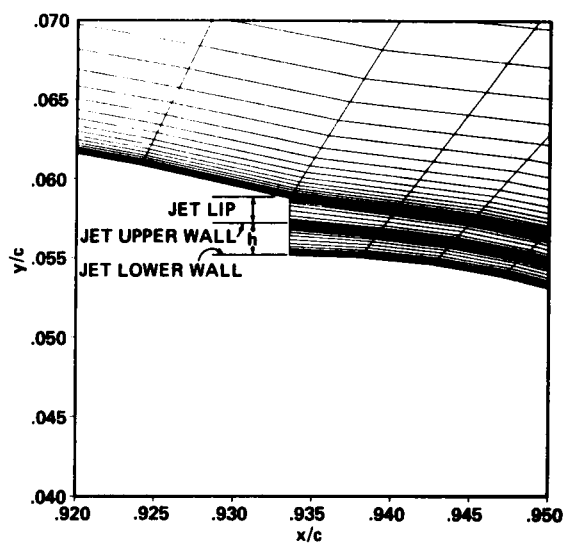


Figure 5.- Grid detail near jet exit; $h/c = 0.002$.

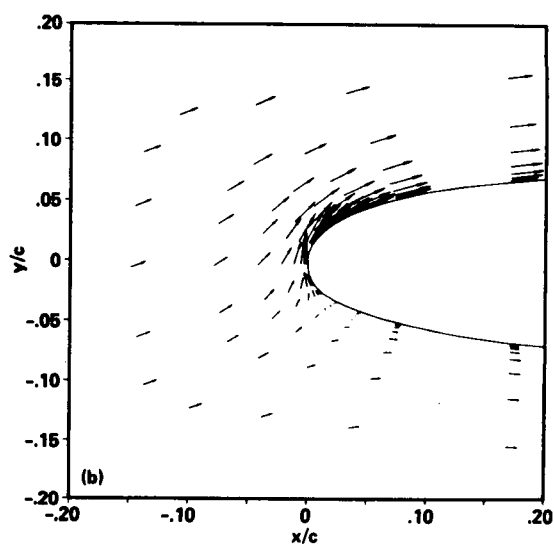
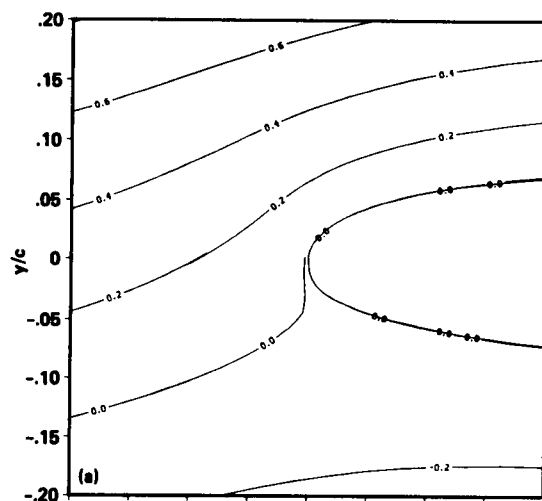


Figure 8.- Stream function and vector field near leading edge of circulation control airfoil. Baldwin-Lomax turbulence model; $C_\mu = 0.03$.
a) Stream function. b) Vector field.

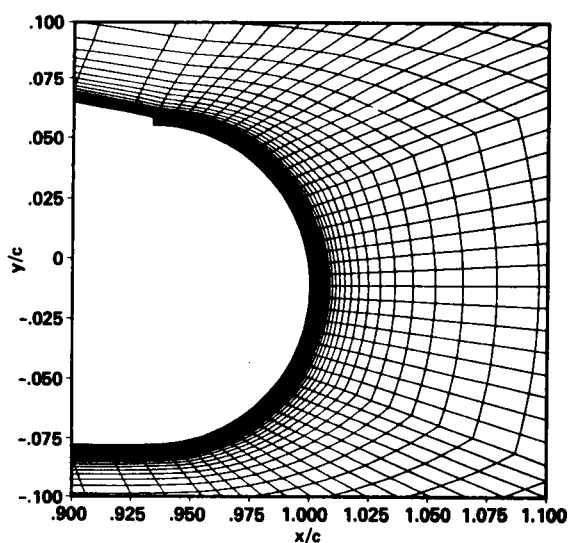


Figure 6.- Grid detail over entire trailing edge.

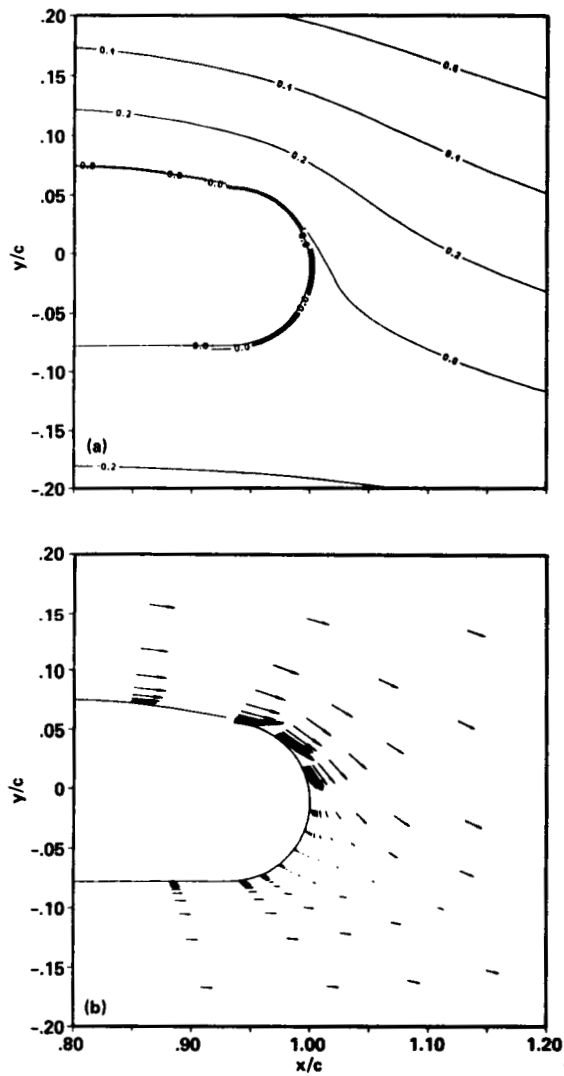


Figure 9.- Stream function and vector field near trailing edge of circulation control airfoil. Baldwin-Lomax turbulence model; $C_\mu = 0.03$. a) Stream function. b) Vector field.

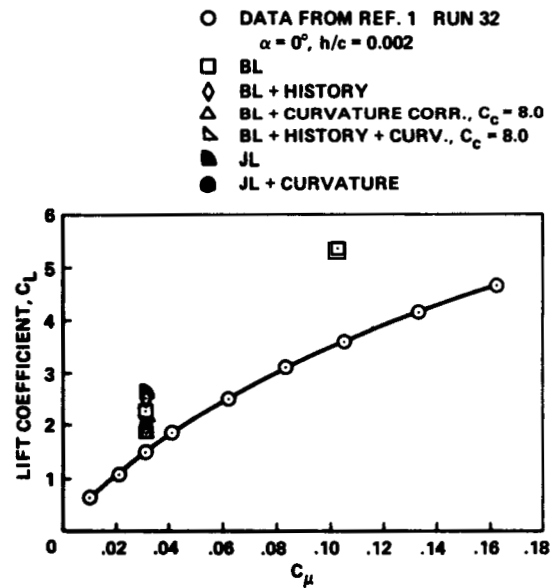


Figure 10.- Sectional lift coefficient as function of jet momentum coefficient. Angle of attack = 0.

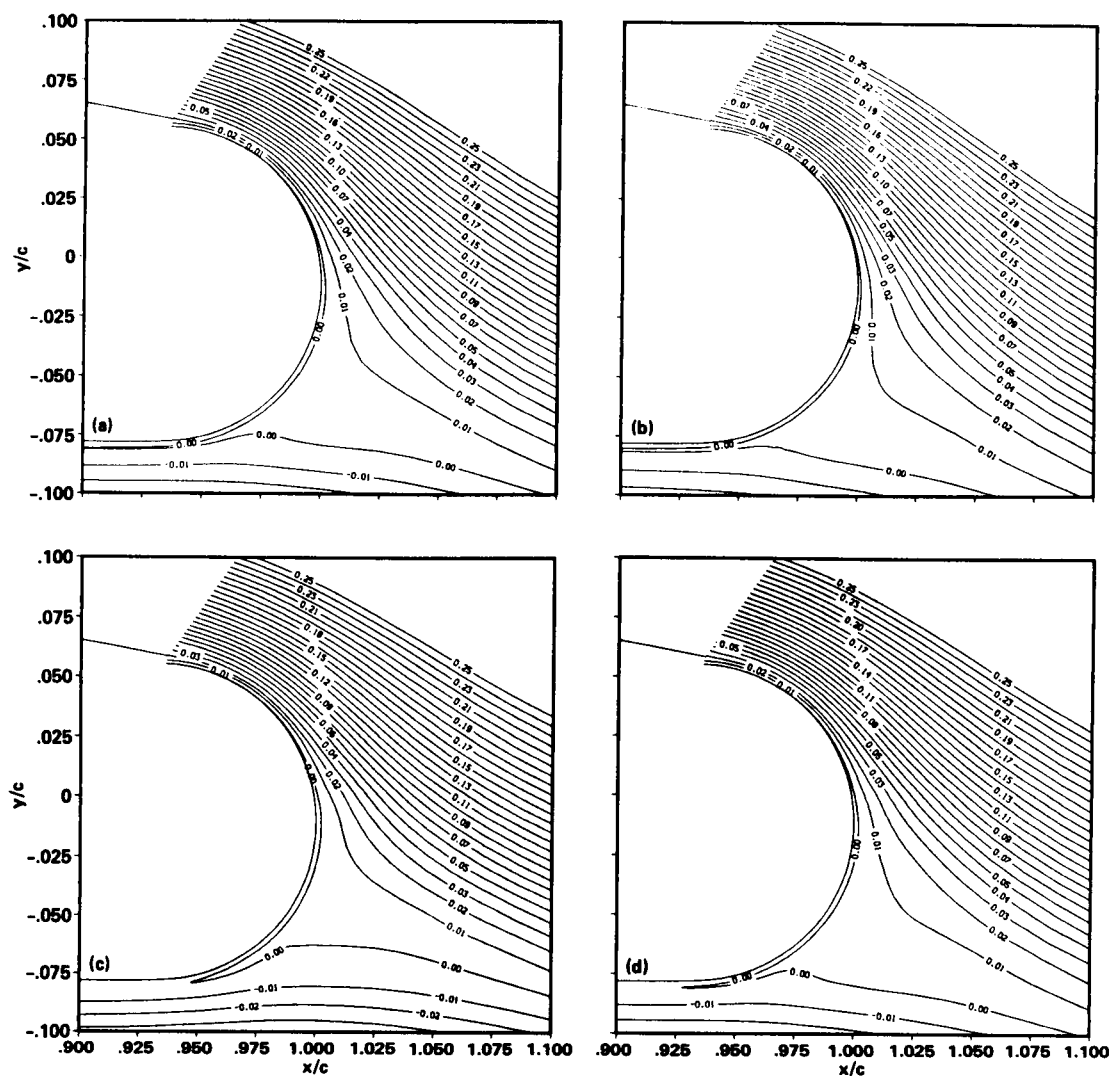


Figure 11.- Stream function corresponding to different turbulence models in the trailing edge region of the circulation control airfoil; $C_u = 0.03$. a) Baldwin-Lomax turbulence model. b) Baldwin-Lomax turbulence model plus jet history. c) Baldwin-Lomax turbulence model plus curvature correction. d) Baldwin-Lomax turbulence model plus jet history and curvature correction.

ORIGINAL PAGE IS
OF POOR QUALITY

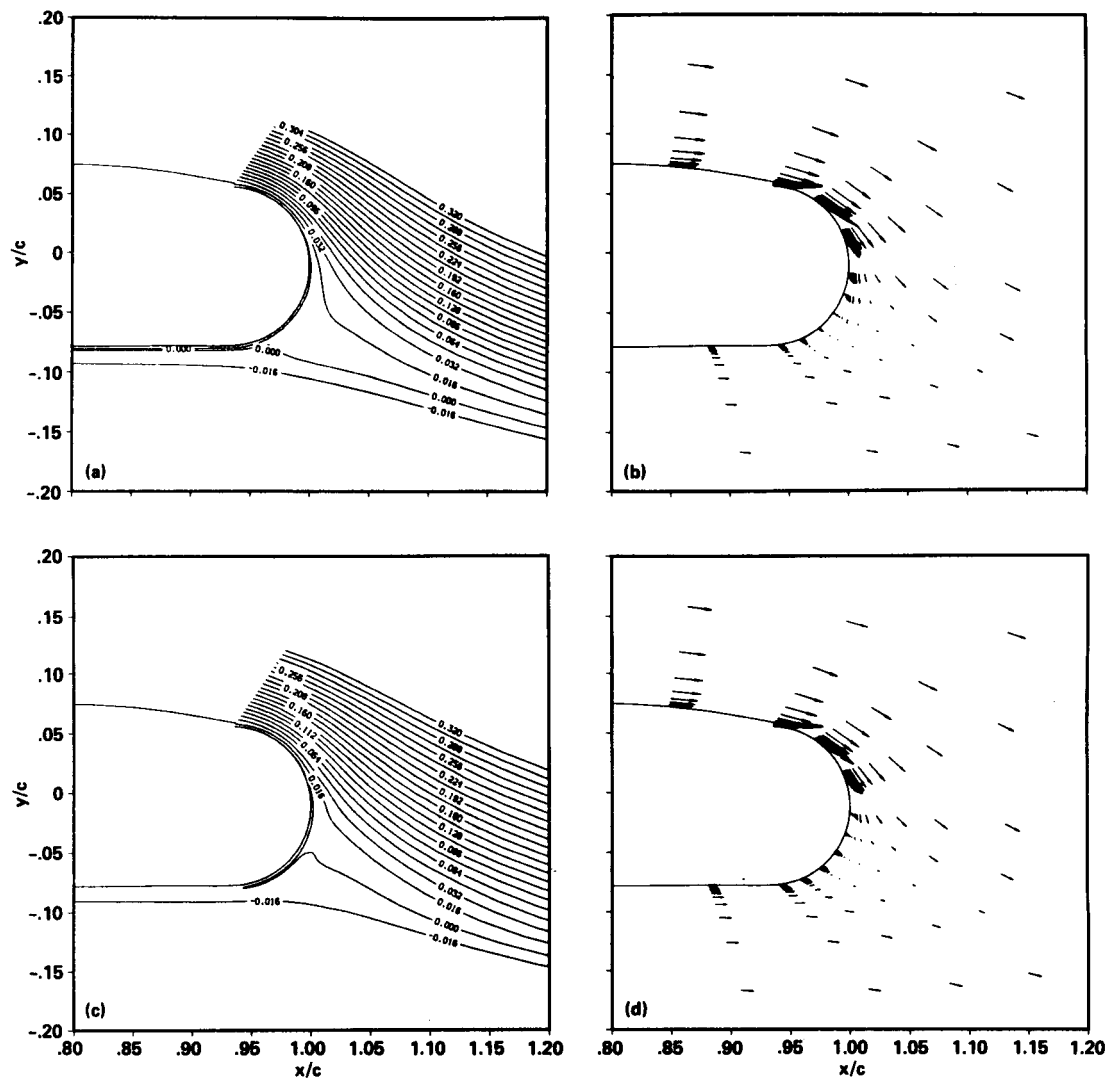


Figure 12.- Stream function and vector field in the trailing-edge region of circulation control airfoil; $C_{\mu} = 0.03$. a) Stream function, Jones-Lauder turbulence model. b) Vector field, Jones-Lauder turbulence model. c) Stream function, Jones-Lauder turbulence model plus curvature correction. d) Vector field, Jones-Lauder turbulence model plus curvature correction.

ORIGINAL PAGE IS
OF POOR QUALITY

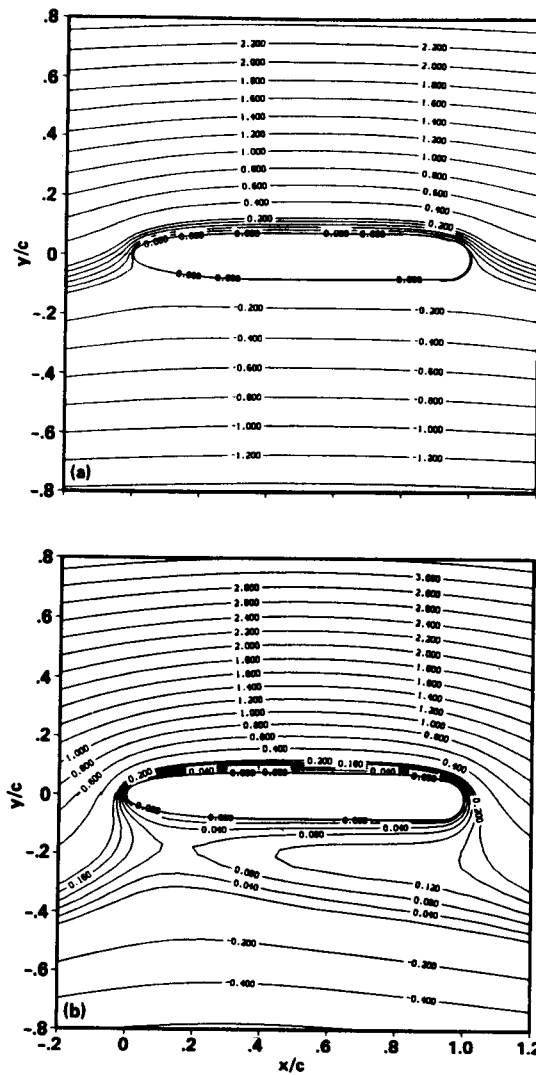


Figure 13.- Comparison of test section stream functions corresponding to two jet mass momentum coefficients. a) $C_\mu = 0.03$. b) $C_\mu = 0.10$.

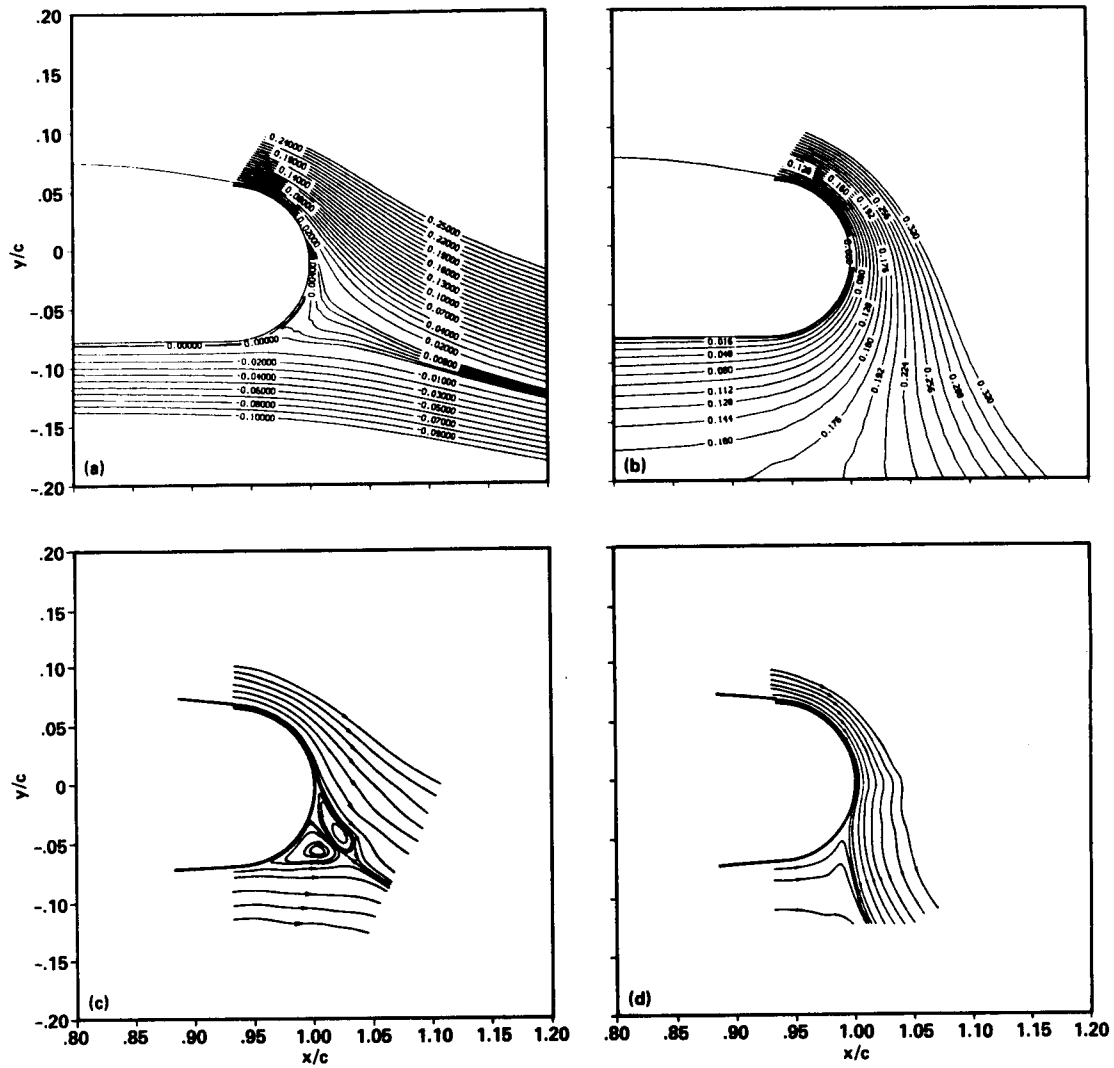


Figure 14.- Comparison of computed and measured streamlines in the trailing-edge region. a) Computed, $C_{\mu} = 0.03$. b) Computed, $C_{\mu} = 0.10$. c) Experimental, $C_{\mu} = 0.03$. d) Experimental, $C_{\mu} = 0.10$.

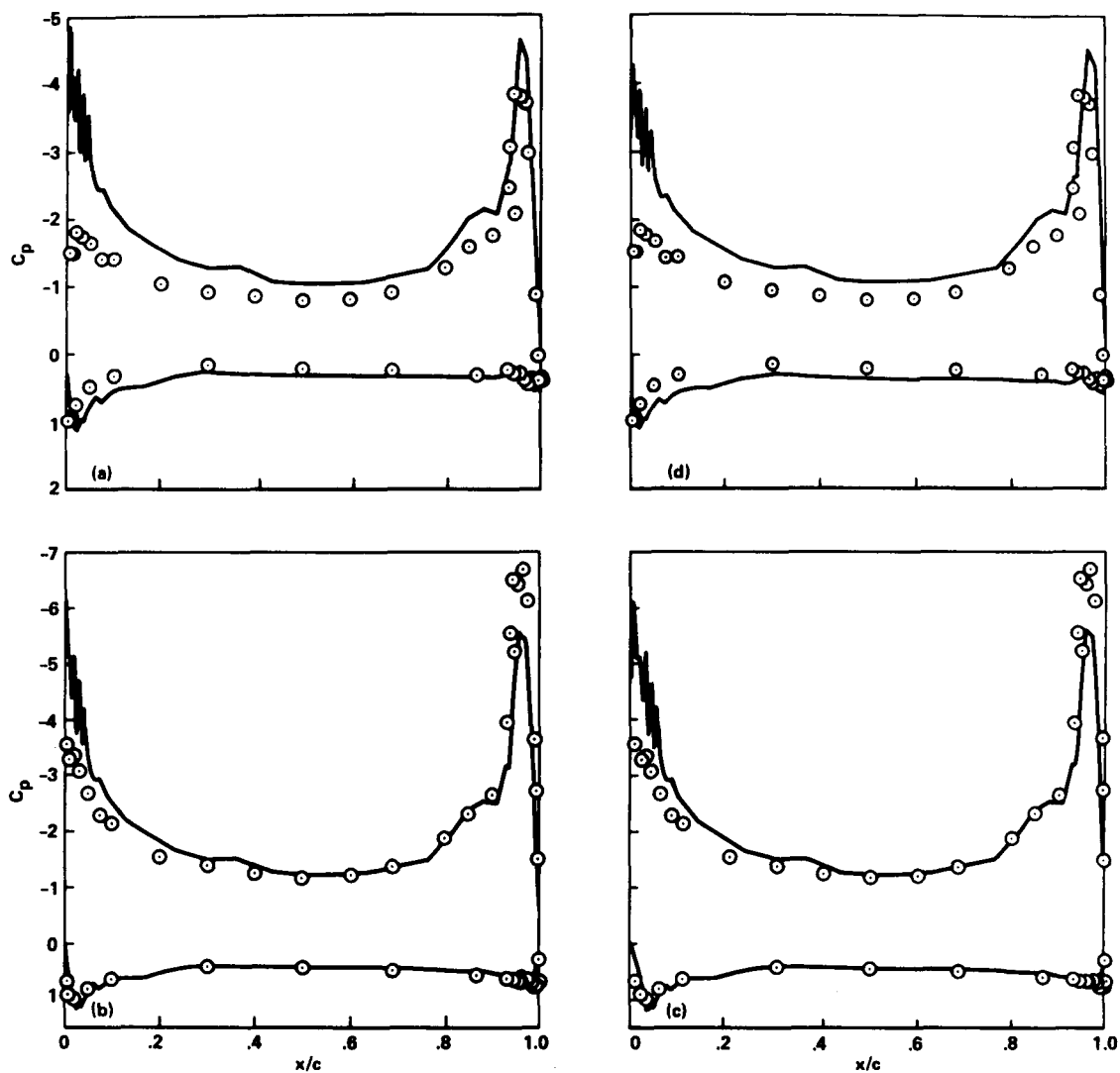


Figure 15.- Pressure coefficient distribution of the upper and lower surfaces of the airfoil. a) Baldwin-Lomax turbulence model plus curvature correction, with jet momentum coefficient matched to the experimental value. b) Baldwin-Lomax turbulence model plus jet history, with total lift matched to the experimental value. c) Jones-Launder turbulence model, with total lift matched to the experimental value. d) Jones-Launder turbulence model corrected for curvature, with jet momentum coefficient matched to the experimental value.

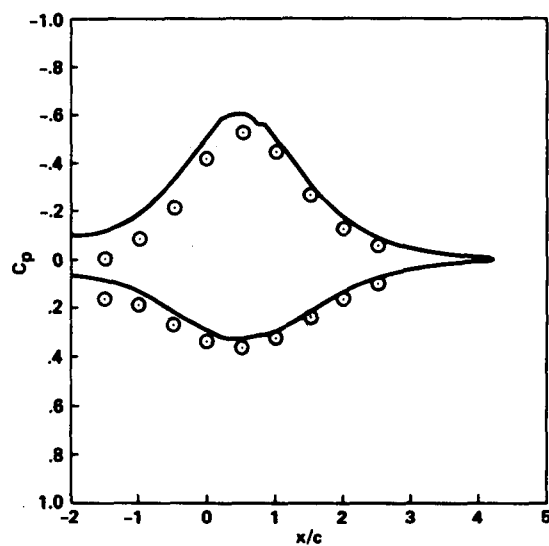


Figure 16.- Comparison of computed and measured pressure coefficients on the upper and lower wind tunnel walls for the Jones-Lauder model with lift matched to the experimental value.

Report Documentation Page

1. Report No. NASA TM-100090		2. Government Accession No.		3. Recipient's Catalog No.	
4. Title and Subtitle On the Validation of a Code and a Turbulence Model Appropriate to Circulation Control Airfoils				5. Report Date April 1988	
				6. Performing Organization Code	
7. Author(s) J. R. Viegas, M. W. Rubesin, and R. W. MacCormack (Stanford University, Stanford, California)				8. Performing Organization Report No. A-88127	
				10. Work Unit No. 505-60-11	
9. Performing Organization Name and Address Ames Research Center Moffett Field, CA 94035				11. Contract or Grant No.	
				13. Type of Report and Period Covered Technical Memorandum	
12. Sponsoring Agency Name and Address National Aeronautics and Space Administration Washington, DC 20546-0001				14. Sponsoring Agency Code	
15. Supplementary Notes Point of Contact: John Viegas, Ames Research Center, MS 229-1 Moffett Field, CA 94035 (415) 694-5950 or FTS 464-5950					
16. Abstract A computer code for calculating flow about a circulation control airfoil within a wind tunnel test section has been developed. This code is being validated for eventual use as an aid to design such airfoils. The concept of code validation being used is explained. The initial stages of the process have been accomplished. The present code has been applied to a low-subsonic, two-dimensional flow about a circulation control airfoil for which extensive data exist. Two basic turbulence models and variants thereof have been successfully introduced into the algorithm, the Baldwin-Lomax algebraic and the Jones-Launder two-equation models of turbulence. The variants include adding a history of the jet development for the algebraic model and adding streamwise curvature effects for both models. Numerical difficulties and difficulties in the validation process are discussed. Turbulence model and code improvements to proceed with the validation process are also discussed.					
17. Key Words (Suggested by Author(s)) Turbulence Circulation control airfoil Code validation			18. Distribution Statement Unclassified-Unlimited Subject Category - 02		
19. Security Classif. (of this report) Unclassified		20. Security Classif. (of this page) Unclassified		21. No. of pages 23	
				22. Price A02	